Hindawi
Journal of Chemistry
Volume 2020, Article ID 1462801, 8 pages
https://doi.org/10.1155/2020/1462801

Research Article

The Influence of Ce or Mn Doping on Cu-Based Catalysts for De-NO_x with NH_3-SCR

Lei Jiang,[1] Yixi Cai,[1] Miaomiao Jin ,[1] Zengzan Zhu,[2] and Yinhuan Wang[2]

[1]*School of Automotive and Transportation Engineering, Jiangsu University, Zhenjiang 212013, China*
[2]*Kailong Lanfeng New Material Technology Co., Ltd., Zhenjiang 212132, China*

Correspondence should be addressed to Miaomiao Jin; miaomiaojin2019@163.com

Received 20 September 2019; Revised 4 March 2020; Accepted 31 March 2020; Published 13 May 2020

Academic Editor: Claudia Crestini

In this study, the de-NO_x performance of Cu-based zeolite catalysts supported on topological structure (SSZ-13, BEA, ZSM-5) and loaded with different doses of copper (from 2 to 6 wt.%) was investigated. The preparation of copper-based catalysts adopted the incipient wetness impregnation method. To analyze the physicochemical properties of the catalysts, advanced techniques like BET, XRD, NH_3-TPD, H_2-TPR, and DRS UV-Vis were used. The performance tests suggested the 4Cu/SSZ-13 catalyst exhibited higher low-temperature activity and wider temperature window. Furthermore, compared with Mn-Cu/SSZ-13, the Ce-Cu/SSZ-13 catalysts exhibited better de-NO_x performance.

1. Introduction

The nitrogen oxide (NO_x) pollution level has caused widespread concern, calling for effective measures to achieve ultralow emission beyond the current efforts. Therefore, urea- (ammonia-) selective catalytic reduction technology (urea-SCR) has been widely employed in removing nitrogen oxide emissions [1]. In recent years, V_2O_5-WO_3/TiO_2 [2, 3] catalysts and copper-based [4–6] and iron-based zeolite [5–8] catalysts have been extensively studied in the NH_3-SCR catalytic system and are gradually being used for commercialization. Vanadium-based catalysts have developed greater sulfur resistance and high NO_x conversion over a broad temperature window, whereas vanadium-based catalysts will lose activity at high temperatures because of the TiO_2 support crystal form. Moreover, the catalyst system contains biologically active component (V_2O_5); then it is easy to sublimate or fall off during the purification process of NO_x from diesel exhaust, which is potentially harmful to the ecological environment and human health. The United States and Japan have already been forbidden the use of vanadium-based catalytic system for NO_x purification of diesel exhaust. Therefore, developing an effective, durable, and environmentally friendly SCR catalyst becomes more important for diesel NO_x removal in the future to replace the traditional vanadium-based catalyst of SCR technology.

SCR zeolitic materials can be divided into straight-channel zeolites (including MFI, BEA, and FAU) and cage type (SSZ-13 and SAPO-34) according to structural characteristics. The main channel of the former SCR reaction is their 3D main channel, whereas the latter is the CHA cage [9–12]. Cu-based zeolite catalysts have attracted extensive focus due to the wide SCR reaction window and excellent N_2 selectivity. However, the upstream process results in poor stability of zeolite in dealumination under severe hydrothermal conditions. The small channel size of SSZ-13 impedes the structural dealumination, and thus possesses higher hydrothermal stability [13].

The molecular sieves for NH_3-SCR catalyst support mainly include ZSM-5, Beta, SSZ-13, SAPO-34, and USY. The CHA structure, especially SSZ-13 molecular sieve, has become the focus of molecular sieve denitration catalyst research and development in recent years due to its exceedingly good de-NO_x performance, N_2 selectivity, and hydrothermal stability [14–16]. Considering that Cu- and Fe-based zeolites catalysts present excellent activity and low cost, they have been very popular with commercial catalyst manufacturers. Wang et al. [17] studied the de-NO_x

performance of fresh and hydrothermal aging (HTA) of Cu- and Fe- based zeolite catalysts and discovered that the Cu/SSZ-13 catalysts exhibited excellent low-temperature performance. Cu/SSZ-13 zeolites were proved to exhibit more excellent durability as compared with other Cu/zeolites by Kwak et al. [18]. It was found by other researchers that Cu/SSZ-13 maintained a high SCR reactivity at 1100 K after16 h hydrothermal treatment [19].

Liu et al. [20] prepared Cu-Mn/SAPO-34 with the incipient witness impregnation method, finding that the NO conversion achieved 72% at 120°C and the de-NO_x performance exceeded 90% when the temperature was up to 180°C. Liu et al. [21] doped Ce and/or Zr over Cu/ZSM-5 zeolite catalysts to study the effect of Ce and/or Zr on the de-NO_x performance using NH_3, and they reported that the high SCR activities of cerium-rich catalysts were caused by the Ce^{3+}/Ce^{4+} redox couple presence. Cerium-containing materials are considered to be of great research value in the application of NO_x emission reduction attributed to the ability to store oxygen and their excellent redox capacity [22, 23]. Overall, the introduction of transition metals and rare earth elements in zeolite catalysts can improve their catalytic performance by changing the active sites and synergistic action (copper) with active components.

In this study, Cu-based zeolite catalysts were prepared by incipient witness impregnation, and their influence on NH_3-SCR reaction was investigated. Furthermore, the optimal type of zeolite was used as a carrier to study the effect of different copper loading on the physicochemical properties of the catalyst and the de-NO_x performance of SCR reaction.

2. Materials and Methods

2.1. Catalyst Preparation. The preparation of all samples is accomplished by the incipient wetness impregnation method. Taking the preparation of the catalysts with 4 wt.% Cu content as an example, the detailed preparation process for different zeolites (BEA, ZSM-5, and SSZ-13) is as follows: first, the water absorption of zeolite (BEA, ZSM-5, and SSZ-13) was tested, and based on its absorption rate, a suitable copper solution was disposed of as an immersion liquid in the required Cu loading amount. The copper solution was quickly and uniformly fixed with the above corresponding zeolite powder. After the zeolite power was stirred 6 times every 5 min when being dried at 100°C, the obtained samples were calcined in the muff furnace at 550°C for 4 h. xCu ($x = 2$, 4, 6 wt.%)/zeolite catalysts were prepared using the same methods.

Doped Cu-M/zeolite (M = cerium/manganese) catalyst powder was prepared by a wetness impregnation method. According to the water absorption rate of SSZ-13, copper and metal loading (1 wt.%), the impregnating solution consists of copper and metallic elements by $Ce(NO_3)_3{\cdot}6H_2O$ (AR,) or $Mn(NO_3)_2$ (50 wt.%) (AR, Sinopharm Chemical Reagent Co., Ltd., China). After impregnating the solution quickly and evenly to the carrier, the samples were dried and calcined under the same conditions as above to get Cu-M/zeolites catalyst powder.

2.2. Activity Measurement. The de-NO_x performance of catalysts was tested by a quartz tubular fixed-bed reactor (i.d. = 24 mm) with 6.28 cm^3 sample (400 mesh), as shown in Figure 1. The catalyst was fixed in the middle of the reaction tube and the tests of the SCR reaction temperature were controlled by the program precision temperature controller (YuDian AI-708). A Mass flowmeter was applied to regulate the concentrations of feed gas. H_2O was provided by a syringe pump (EverSeiko, 022 Pulsation Control Single) and mixed with the feed gas in the evaporator.

The simulation gas was composed of 500 ppm NO, 550 ppm NH_3, 8 vol% O_2, 5 vol% CO_2, 5 vol% H_2O, and N_2 balance (300 mL/min). The gas hourly space velocity (GHSV) value was kept about 50,000 h^{-1}. Typically, a mass flow controller was used to control the gas composition. The NO_x conversion (X_{NO_x}) and N_2O yield (X_{N_2O})evaluated the catalyst activities and selectivity by using the following equation:

$$X_{NO_x} = \frac{[NO_x]_{in} - [NO_X]_{out}}{[NO_x]_{in}} \times 100\%,$$
$$X_{N_2O} = \frac{2N_2O}{[NH_3]_{in} + [NO]_{in}} \times 100\%. \quad (1)$$

2.3. Catalyst Characterization. Brunauer–Emmett–Teller (BET) and Barrett–Jioner–Halenda (BJH) methods were utilized to evaluate the specific surface area, the pore volume, and the average pore diameter in the experiments. The physical characteristics of parent zeolites and copper-based zeolites previously degassed at 200°C for 6 h were measured based on nitrogen adsorption performed on a Quantachrome NOVA2000-e analyzer.

The X-ray diffraction (XRD) was operated using a Bruker D8-ADVANCE device with Ni filter and Cu-Kα radiation ($\lambda = 0.15418$ nm 40 kV × 200 mA) at room temperature with a scanning velocity of 5°/min ($2\theta = 20$ to 80°). Data were processed with the JADE 6.5 software.

The NH_3-temperature-programmed desorption (NH_3-TPD) experiment was performed with a CHEMBET 3000 chemical adsorption instrument (Quantachrome.). In the NH_3-TPD experiment, a sample of 0.2 g was taken and fixed at the bottom of the U-shaped quartz reactor. In order to remove the surface impurities, the pretreatment was carried out in pure argon (Ar) under 500°C for 30 min and then cooled at 45°C, after which the gas composition was changed into a NH_3/N_2 for adsorption. When the thermal conductivity detector (TCD) baselines were stable, the gas composition was switched to N_2 again for removal of surface physically adsorbed NH_3. After attaining the stability of TCD baselines, the temperature increased to 850°C in N_2 atmosphere by a rate of 10°C/min, and NH_3 desorption was detected by TCD. The standard signal peak of a certain amount of NH_3 was calibrated with a quantitative loop, and the amount of NH_3 desorption of different samples was quantitatively calculated at corresponding temperatures by comparison.

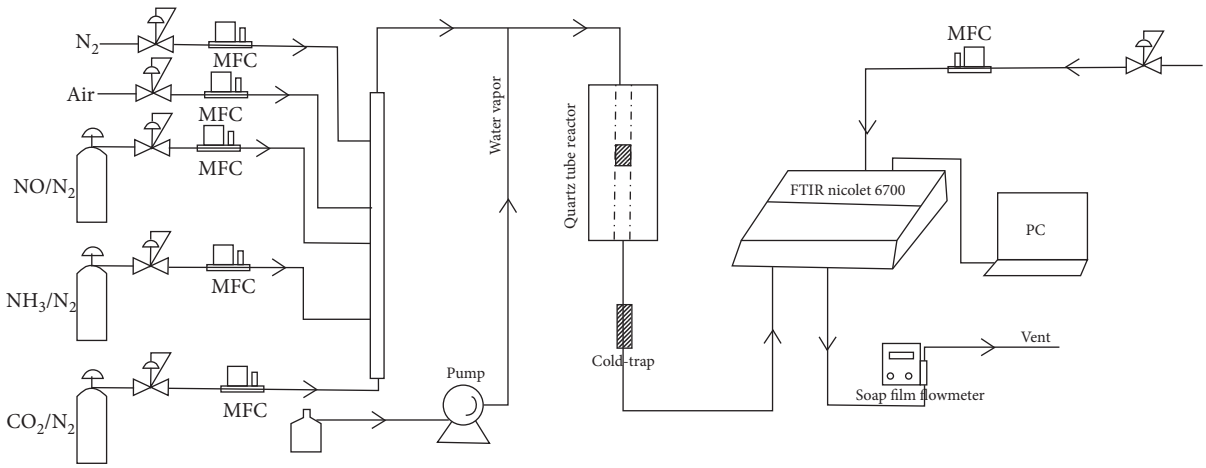

Figure 1: Activity evaluation simulation gas test platform.

The H_2-temperature programmed reduction (H_2-TPR) experiments were conducted with Quantachrome. Firstly, pretreatment of the catalyst was performed at 500°C for 30 min in pure Ar atmosphere in order to remove the surface impurities and then cooled to below 30°C. Then, the atmosphere was switched to a 10% H_2/N_2 mixture. When TCD baselines become stable, the temperature increased to 950°C under the same atmosphere by a rate of 10°C/min. After the exhaust was dehydrated by zeolite, the hydrogen consumption was detected by TCD.

The UV-Vis spectroscopy was operated on a SHIMADZU UV-2600 device to evaluate the nuclearity status of the copper species in the zeolite with different Cu loadings. The reflectance spectra ranging from 200 to 900 nm (wavelength) was recorded using $BaSO_4$ as reference sample.

3. Results and Discussion

3.1. BET Analysis. Table 1 shows the BET results. It could be seen that the purified SSZ-13 had larger surface area and average pore diameter and pore volume than copper-containing zeolites. The surface area and pore volumes of samples were reduced when copper was added to the zeolite, which indicated that the internal pores of zeolites were covered or permeated by copper species. The SSZ-13 zeolites were in the micropore range.

3.2. XRD Patterns. The crystal structures and phase composition of *x*Cu/SSZ-13 ($x = 2$, 4, 6 wt.%) were investigated by powdered XRD measurements, and the XRD patterns are exhibited in Figure 2. Peaks of all samples were observed at $2\theta = 20.9°$, 23.5°, 25.4°, 26.3°, 28.1°, 28.6°, 31.0°, 31.5°, and 35.0°, associated with typical chabazite (CHA) structure [13]. Futhermore, the XRD pattern of the Cu/SSZ-13 was not detected for diffraction peaks of CuO_x ($2\theta = 35.4°$ and 36.5°); this observation suggested that the copper species presented a good dispersion on the surface of the zeolite or the Cu loadings in the samples used in this work were so low that they could not be determined [24].

3.3. NH_3-TPD Analysis. The acidity of zeolitic materials has an important impact on the extent of NO_x reduction, and NH_3-TPD could be employed to analyze the acidity of Cu/zeolites. NH_3 peaks at 134°C, 194°C, and 537°C were observed in Figure 3 for all the samples. The NH_3 desorption peaks at 134°C were assigned to loosely bound NH_3 species, desorption peaks at 194°C were attributed to NH_3 adsorbed on Cu^{2+} ions, and the NH_3 released from the Brønsted acid sites was responsible for the lowest peaks observed at higher than 500°C [25]. Compared with the different copper content SSZ-13 zeolites, the peaks presented the strongest NH_3 desorption from the Cu^{2+} ions after Cu was loaded 4 wt.% at 194°C. This result suggested 4% Cu/SSZ-13 catalyst had a higher acid strength than the other two catalysts [10, 26].

Then, it can be concluded that the rise of copper loading could contribute to adding moderate acid intensity, which could have a promotional effect on the adsorption of NH_3. When the copper loading in the sample increased to 4%, the strength of acid reached the maximum. With further increasing the Cu loading, Lewis acid sites decreased. The NH_3-TPD results showed that the stronger Lewis acid in the 4% Cu/SSZ-13 catalyst possibly possess a higher activation capacity of NH_3.

3.4. H_2-TPR Results. Reducibility and distribution of copper species in the *x*Cu/SSZ-13 catalysts were investigated by H_2-TPR. Figure 4 exhibi two reduction peaks of 2% Cu/SSZ-13 and 4% Cu/SSZ-13 at 215°C and 413°C and shows one peak of 6% Cu/SSZ-13 at 193°C. Peak A at 215°C was probably related to the reduction of Cu^{2+} in the SSZ-13 zeolite structure (CHA cages). Peak B was attributed to that the Cu^+ ions could be reduced to metallic Cu at 413°C. It can be observed from Figure 4 that Cu^{2+} and CuO reduction peaks were increased clearly when increasing the content of copper, while no effect was observed on the reduction peak of Cu^+ because of insignificant production of copper oxide species. In addition, the reduction temperature decreased with increasing Cu loadings, indicating the redox ability increased with increasing Cu loadings of Cu-SSZ-13. This

Table 1: Physical characteristics of Cu/SSZ-13 zeolites.

Samples	Specific area (m^2/g)	Pore volume (cm^3/g)	Pore diameter (nm)
SSZ-13	553	0.2966	1.914
2% Cu/SSZ-13	549	0.2875	1.913
4% Cu/SSZ-13	517	0.2794	1.902
6% Cu/SSZ-13	493	0.2769	1.900

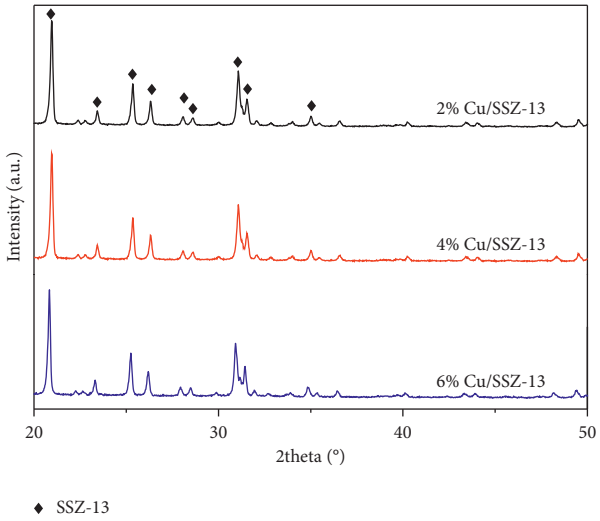

Figure 2: XRD patterns of the xCu/SSZ-13 ($x = 2$, 4, 6%) catalysts.

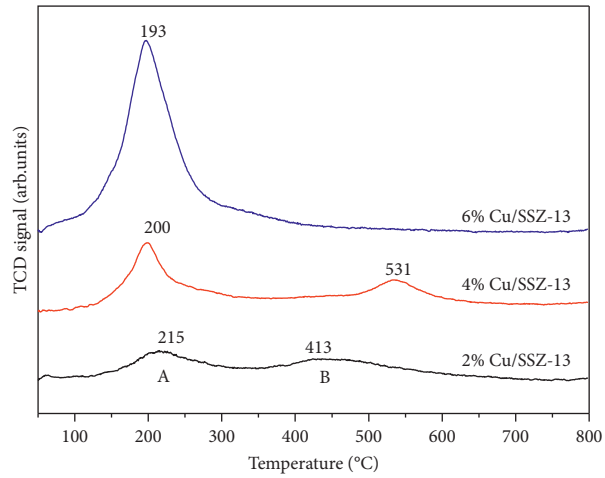

Figure 4: TPR patterns of xCu/SSZ-13 ($x = 2$, 4, and 6%) catalysts.

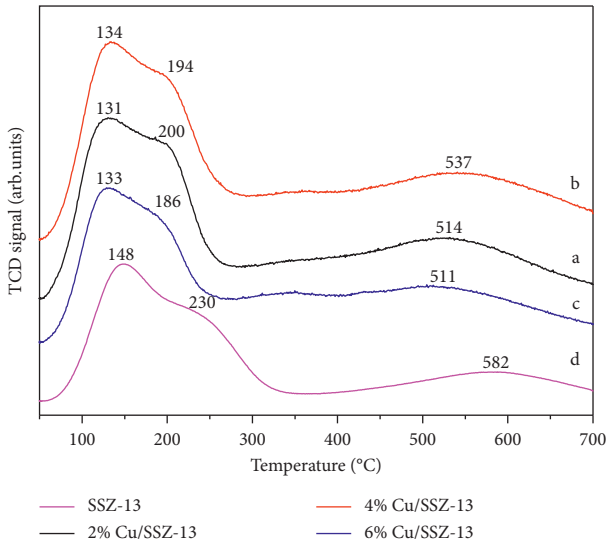

Figure 3: NH_3-TPD profile of copper-modified SSZ-13 catalysts: (a) 2% Cu/SSZ-13, (b) 4% Cu/SSZ-13, (c) 6% Cu/SSZ-13, and (d) SSZ-13.

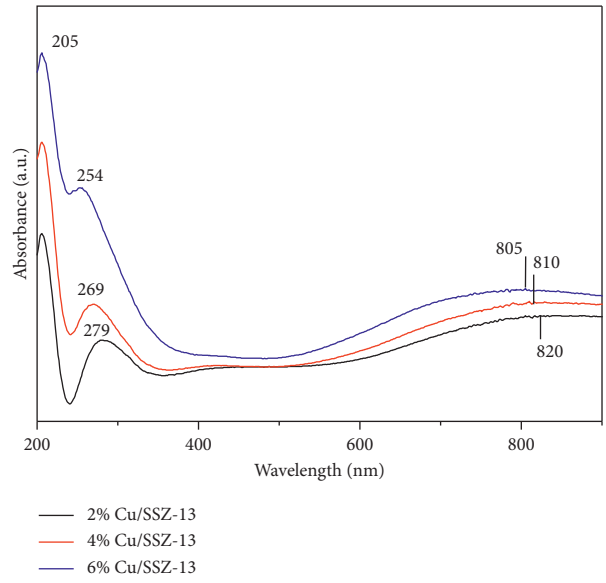

Figure 5: UV-Vis DRS spectra of the Cu/SSZ-13 ($x = 2$, 4, 6%) catalysts.

high redox ability would lead to the nonselective oxidation of NH_3, resulting in a relatively poorer SCR activity and N_2 selectivity of Cu-SSZ-13 with high Cu contents at high temperatures [27].

3.5. DRS UV-Vis. UV-Vis-DRS spectra are shown in Figure 5, which provided us an insight into the copper species in the SSZ-13 zeolites. The band at approximately 810 nm and around 254 nm could be derived from the d-d transition in isolated Cu (II). The peak at around 254 nm was assigned to the charge transfer of $O^{2-} \longrightarrow Cu^{2+}$ transition from lattice oxygen; the band range of 380–600 nm could be ascribed to transition of Cu_xO ($[Cu\text{-}O\text{-}Cu]^{2+}$ and CuO species). And, those bands at around 560 nm and above are related to the Cu^{2+} where

electronic d-d transitions took place within a distorted octahedral structure in CuO particles with oxygen around it. The different copper contents in the catalysts could cause variations of peaks in different degrees in the DRs UV-Vis results. It was found that the 6% Cu/SSZ-13 catalyst showed the highest intensity at the bands of 254 nm. Overall, this results is similar to phenomenon with the different copper oxide contents from H_2-TPR curves, due to that the band strength of copper oxide species increases with the content of Cu loading.

3.6. NOx Conversion of Cu/Zeolite. Figure 6 exhibits the NO conversion of different zeolites by comparing ZSM-5, BEA, and SSZ-13. Cu/SSZ-13 catalyst presented the highest de-NOx performance and the lowest ignition temperature, and the SCR active centers were in the form of larger number of stable single Cu2+ in the CHA (Chabazite) cages. In addition, Cu/SSZ-13 catalyst always maintained the high activity up to 520°C (NOx conversion >98%), and 2 wt.% Cu/SSZ-13 sample possessed greater activity up to full conversion at 250°C. This is because the NOx reduction was dependent on cage structure as well as exhibiting the active window in an obvious broadening. It was observed that for Cu/ZSM-5 and Cu/BEA zeolite catalysts, the low-temperature performance was noticeably worse, and especially for Cu/BEA catalyst NOx, conversion capability reached nearly 98% at 370°C. As the temperature increased, the conversion rate dropped rapidly and had dropped below 80% at 470°C. A catalyst had narrow active temperature window (230~460°C) with poor performance at low temperature.

In general, the catalysts of copper loading on SSZ-13 zeolites possessed low ignition temperature, wide active window, and good hydrothermal stability.

3.7. Effect of Cu Loading. Figure 7(a) exhibits the NO conversion of the catalysts with different Cu loadings on SSZ-13 zeolites. The samples had Cu-concentration in the range of 2~6 wt.%. Firstly, at low-temperature (<270°C), the NO conversion was related to copper concentration. The Cu content from 2 wt.% to 6 wt.% improved the low-temperature activity and possessed lower ignition temperature. In case of 6 wt.% Cu/SSZ-13, a particular performance was observed, when the NO conversion was around 20% at 100°C, whereas the NO conversion achieved highest (almost 100% of NOx conversion) at 206°C. When the reaction temperature increased to 407°C, obviously a decrease in the NO conversion was observed within the active window range 300°C. As a comparison, the 4 wt.% copper was loaded on SSZ-13, low-temperature activity to catalyst was moderated, and the NOx conversion achieved highest at 250°C. The NO conversion was around highest at 250°C and remained high in a wide temperature range (almost 100% of NOx conversion). When temperature increased to 460°C, the de-NOx conversions gradually decreased. This decline was principally related to NH3 oxidation competition reaction, and oxidation reaction produces NOx at high temperature. For minimum copper content catalyst (2 wt.%), the de-NOx conversions were completely achieved until temperature reached 270°C with poor low-temperature

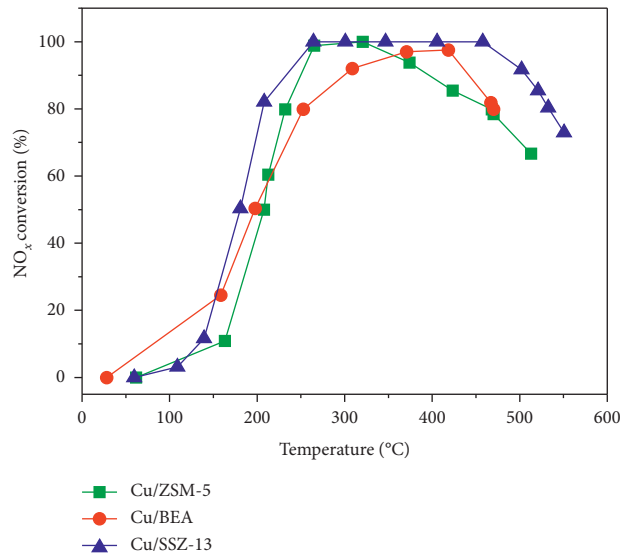

Figure 6: Comparison of SCR activity on Cu with different zeolites.

activity. Therefore, the copper loading was up to 4 wt.%, which possessed the great de-NOx performance at low-temperatures and widest active temperature window, which had the best comprehensive de-NOx performance. In addition, the N2O formation should also be taken into account. Figure 7(b) displays N2O outlet concentrations at different reaction temperatures. One local maximum at 200–300°C is found for each sample. The 6% Cu/SSZ-13 catalyst generates the highest N2O concentration, reaching 5.6 ppm at 254°C; the N2O formation decreased as the copper content declined from 6% to 2% over the temperature range from around 150 to 350°C. Although 2% Cu/SSZ-13 generates the lowest N2O concentration, it is noted that there is a slight difference between the N2O concentration generated by 2% Cu/SSZ-13 and 4% Cu/SSZ-13, which is far lower than 6% Cu/SSZ-13 catalyst.

3.8. Influence of Ce or Mn Doping over Cu/SSZ-13. Figure 8 shows the NO_x conversion on all the samples from 50 to 600°C. Doping cerium and manganese over Cu/SSZ-13 catalysts, respectively, were simultaneously impregnated. Before doping with cerium or manganese to Cu/SSZ-13, the poor low temperature performance of the catalyst was exhibited, and the high light-off temperature was presented. Whether doped with cerium or manganese, the low-temperature performance of the catalyst was significantly improved, and the light-off temperature dropped to 167°C. Cu-Mn-SSZ-13 catalyst had a better NO oxidation activity because doping Mn promoted the oxidation of Cu^+ to Cu^{2+}, but the surface area decreased after Mn was doped [28]. Ce could add the number of the isolated Cu^{2+} species and promote the formation of the bidentate nitrate species [29]. The addition of cerium, compared with doping manganese, exhibited broadening active window at higher temperatures, and the NO_x conversion reached 80% at lower temperature, which suggested that the influence of doping cerium over the

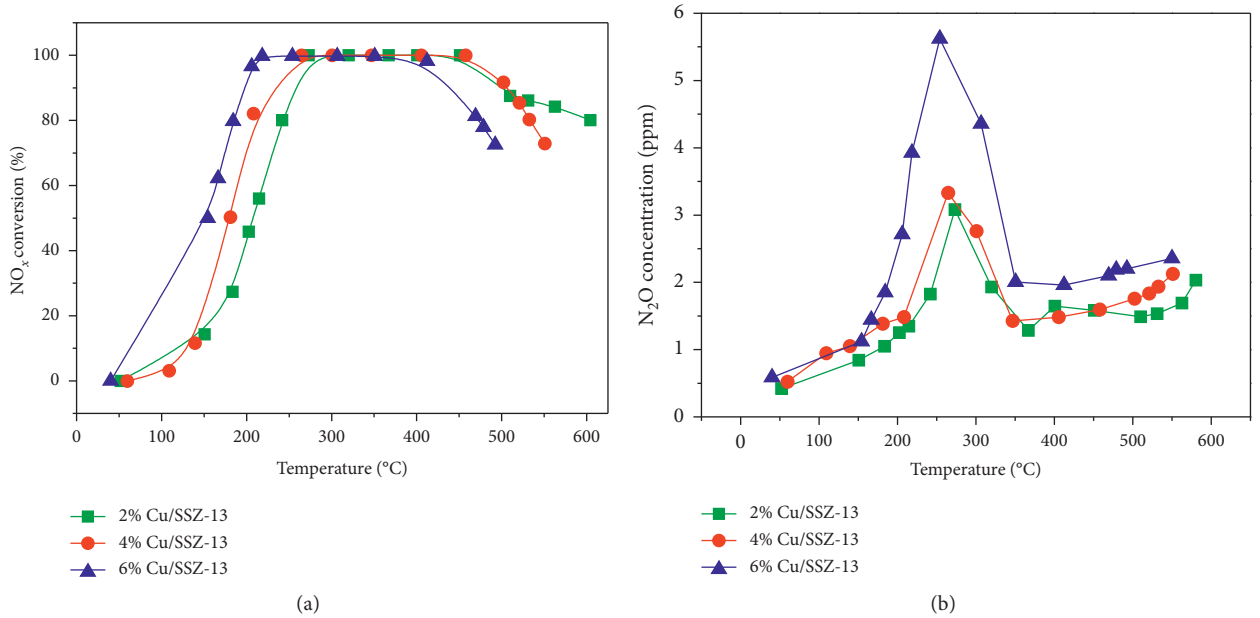

Figure 7: (a) SCR activity of the catalysts; (b) N_2O concentration during NH3-SCR with xCu/SSZ-13 (x = 2, 4, 6%) catalysts.

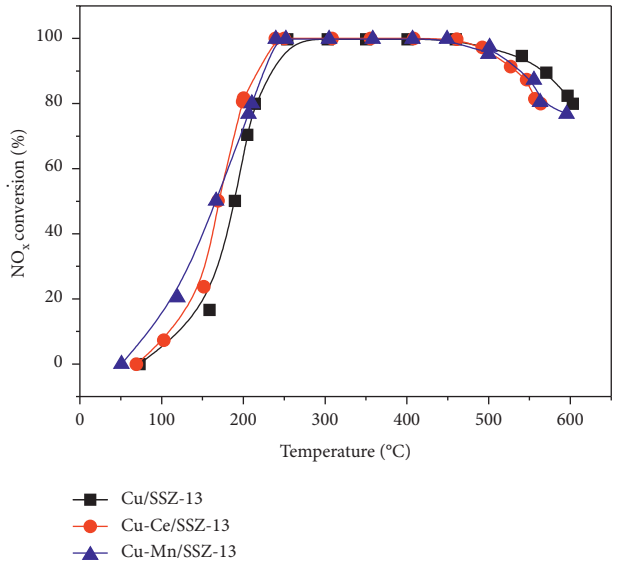

Figure 8: NO_x conversion using NH_3 for addition of Ce or Mn on Cu/SSZ-13 catalysts.

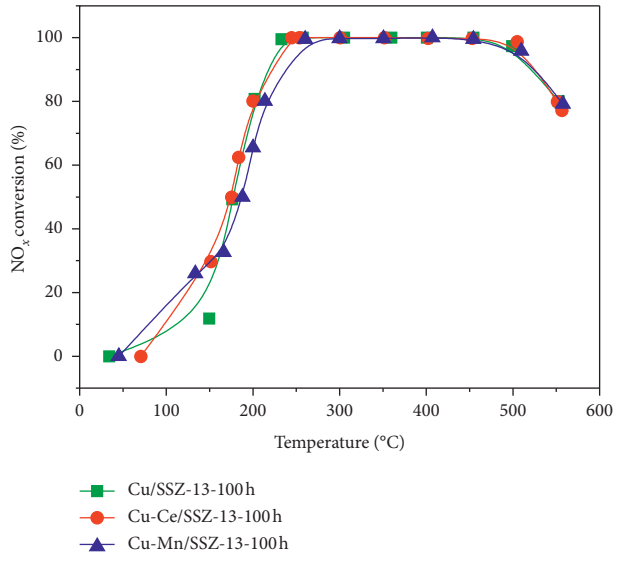

Figure 9: NO_x conversion after aging treatment for 100 h using NH_3 for addition of Ce or Mn on Cu/SSZ-13 catalysts.

catalysts was more significant. Doping Ce promoted the low-temperature catalytic performance with increasing NO_x reduction rate.

The doping manganese in Cu/SSZ-13 presented poorer resistance to hydrothermal aging as can be observed in Figure 9. The low-temperature activity deteriorated, and the light-off temperature increased after hydrothermal aging for 100 hours, corresponding to active temperature window narrowing. Ce-doped sample showed the activity temperature window similar to the undoped sample. However, the doping of Ce significantly improved the low-temperature activity of the catalyst. For example, NO_x conversion reached 20% at 100°C, whereas the temperature increased to 160°C; the undoped Cu/SSZ-13 catalysts achieved the same conversion. The doped Ce in catalysts maintained the structural characteristics of the hydrothermal aging catalyst surface. Compared with Cu/SSZ-13 catalyst, the addition of Ce stabilized the copper active center and reduced the SSZ-13 structure dealuminization, which kept the Cu-Ce-SSZ-13 catalysts possessing excellent hydrothermal stability [28].

According to the above analysis, the rare earth element Ce, as an ideal molecular sieve-based SCR catalyst

modification element, could significantly improve the low-temperature performance of the catalyst and broaden the temperature window.

4. Conclusions

In this paper, Cu-based zeolite catalysts were investigated in terms of NO_x conversion using NH_3 under the atmospheres of N_2, O_2, NO, NH_3, CO_2, and H_2O. It has been found that the zeolite topologies, Cu loadings, and transition metal doping affect the catalytic performance with regard to NO_x conversion. The SSZ-13 possessed a small pore and exhibited the optimal SCR activity because of existing high single Cu^{2+} species in the pores.

The Cu_x/SSZ-13 catalysts prepared with wetness impregnation possess dispersed Cu^{2+} species, Cu_xO_y clusters, and CuO particles, compared with 6% Cu/SSZ-13 and 2% Cu/SSZ-13. 4% Cu/SSZ-13 demonstrated the best catalytic activity under low temperature, the widest active temperature window, and the highest comprehensive SCR de-NO_x performance. Doping rare earth element Ce could effectively improve the low-temperature de-NO_x performance of the catalysts and broaden the reaction temperature window.

Data Availability

The data used to support the findings of this study are included within the article.

Conflicts of Interest

The authors declare no conflicts of interest.

Acknowledgments

This research was funded by the Key Research Program of Jiangsu Province, China, grant number BE2016003-2.

References

[1] F. Liu, H. He, C. B. Zhang et al., "Selective catalytic reduction of NO with NH_3 over iron titanate catalyst: catalytic performance and characterization," *Applied Catalysis B Environmental*, vol. 96, no. 3-4, pp. 408–420, 2010.

[2] P. G. W. A. Kompio, A. Brückner, F. Hipler, G. Auer, E. Löffler, and W. Grünert, "A new view on the relations between tungsten and vanadium in V_2O_5-WO_3/TiO_2 catalysts for the selective reduction of NO with NH_3," *Journal of Catalysis*, vol. 286, pp. 237–247, 2012.

[3] Y. Dong and X. Fei, "Effect of isopropanol on crystal growth and photocatalytic properties regulation of anatase TiO_2 single crystals," *Materials Technology*, vol. 35, no. 2, pp. 102–111, 2020.

[4] I. E. Wachs, G. Deo, B. M. Weckhuysen et al., "Selective catalytic reduction of NO with NH_3 over supported vanadia catalysts," *Journal of Catalysis*, vol. 161, no. 1, pp. 211–221, 1996.

[5] G. Busca, L. Lietti, G. Ramis, and F. Berti, "Chemical and mechanistic aspects of the selective catalytic reduction of NO_x by ammonia over oxide catalysts," *Applied Catalysis B: Environmental*, vol. 18, no. 1-2, pp. 1–36, 1998.

[6] J. Li, H. Chang, L. Ma, J. Hao, and R. T. Yang, "Low-temperature selective catalytic reduction of NO_x with NH_3 over metal oxide and zeolite catalyst," *Catalysis Today*, vol. 175, no. 1, pp. 147–156, 2011.

[7] T. V. W. Janssens, H. Falsig, L. F. Lundegaard et al., "A consistent reaction scheme for the selective catalytic reduction of nitrogen oxides with ammonia," *ACS Catalysis*, vol. 5, no. 5, pp. 2832–2845, 2015.

[8] S. Brandenberger, O. Kröcher, A. Tissler, and R. Althoff, "The state of the art in selective catalytic reduction of NO_x by ammonia using metal-exchanged zeolite catalysts," *Catalysis Reviews*, vol. 50, no. 4, pp. 492–531, 2008.

[9] L. Xie, F. Liu, L. Ren, X. Shi, F.-S. Xiao, and H. He, "Excellent performance of one-pot synthesized Cu-SSZ-13 catalyst for the selective catalytic reduction of NO_x with NH_3," *Environmental Science & Technology*, vol. 48, no. 1, pp. 566–572, 2014.

[10] J. Wang, T. Yu, X. Wang et al., "The influence of silicon on the catalytic properties of Cu/SAPO-34 for NO_x reduction by ammonia-SCR," *Applied Catalysis B: Environmental*, vol. 127, pp. 137–147, 2012.

[11] A. Sultana, T. Nanba, M. Sasaki, M. Haneda, K. Suzuki, and H. Hamada, "Selective catalytic reduction of NO_x with NH_3 over different copper exchanged zeolites in the presence of decane," *Catalysis Today*, vol. 164, no. 1, pp. 495–499, 2011.

[12] B. Chen, R. Xu, R. Zhang, and N. Liu, "Economical way to synthesize SSZ-13 with abundant ion-exchanged Cu^+ for an extraordinary performance in selective catalytic reduction (SCR) of NO_x by ammonia," *Environmental Science & Technology*, vol. 48, no. 23, pp. 13909–13916, 2014.

[13] P. G. Blakeman, E. M. Burkholder, H.-Y. Chen et al., "The role of pore size on the thermal stability of zeolite supported Cu SCR catalysts," *Catalysis Today*, vol. 231, pp. 56–63, 2014.

[14] C. Niu, X. Shi, F. Liu et al., "High hydrothermal stability of Cu-SAPO-34 catalysts for the NH_3-SCR of NO_x," *Chemical Engineering Journal*, vol. 294, pp. 254–263, 2016.

[15] Y. Ma, X. Wu, J. Zhang, R. Ran, and D. Weng, "Urea-related reactions and their active sites over Cu-SAPO-34: formation of NH_3 and conversion of HNCO," *Applied Catalysis B: Environmental*, vol. 227, pp. 198–208, 2018.

[16] C. Fan, Z. Chen, L. Pang et al., "Steam and alkali resistant Cu-SSZ-13 catalyst for the selective catalytic reduction of NO_x in diesel exhaust," *Chemical Engineering Journal*, vol. 334, pp. 344–354, 2018.

[17] A. Wang, Y. Wang, E. D. Walter et al., "NH_3-SCR on Cu, Fe and Cu plus Fe exchanged beta and SSZ-13 catalysts: hydrothermal aging and propylene poisoning effects," *Catalysis Today*, vol. 320, pp. 91–99, 2019.

[18] J. H. Kwak, D. Tran, S. D. Burton, J. Szanyi, J. H. Lee, and C. H. F. Peden, "Effects of hydrothermal aging on NH_3-SCR reaction over Cu/zeolites," *Journal of Catalysis*, vol. 287, pp. 203–209, 2012.

[19] J. H. Kwak, R. G. Tonkyn, D. H. Kim, J. Szanyi, and C. H. F. Peden, "Excellent activity and selectivity of Cu-SSZ-13 in the selective catalytic reduction of NO_x with NH_3," *Journal of Catalysis*, vol. 275, no. 2, pp. 187–190, 2010.

[20] G. Liu, W. Zhang, P. He et al., "H_2O and/or SO_2 tolerance of Cu-Mn/SAPO-34 catalyst for NO reduction with NH_3 at low-temperature," *Catalysts*, vol. 9, no. 3, p. 289, 2019.

[21] Y. Liu, C. Song, G. Lv, C. Lv, and X. Li, "Promotional effect of cerium and/or zirconium doping on Cu/ZSM-5 catalysts for selective catalytic reduction of NO by NH_3," *Catalysts*, vol. 8, no. 8, p. 306, 2018.

[22] R. Zhang, W. Y. Teoh, R. Amal, B. Chen, and S. Kaliaguine, "Catalytic reduction of NO by CO over Cu/CexZr$1_{1-x}O_2$

prepared by flame synthesis," *Journal of Catalysis*, vol. 272, no. 2, pp. 210–219, 2010.

[23] M. L. Fu, X. H. Yue, D. Q. Ye et al., "Soot oxidation via CuO doped CeO_2 catalysts prepared using coprecipitation and citrate acid complex-combustion synthesis," *Catalysis Today*, vol. 153, no. 3-4, pp. 125–132, 2010.

[24] L. Ma, Y. Cheng, G. Cavataio, R. W. McCabe, L. Fu, and J. Li, "Characterization of commercial Cu-SSZ-13 and Cu-SAPO-34 catalysts with hydrothermal treatment for NH_3-SCR of NO_x in diesel exhaust," *Chemical Engineering Journal*, vol. 225, pp. 323–330, 2013.

[25] H. Wang, R. Xu, Y. Jin, and R. Zhang, "Zeolite structure effects on Cu active center, SCR performance and stability of Cu-zeolite catalysts," *Catalysis Today*, vol. 327, pp. 295–307, 2019.

[26] Y. Li, J. Deng, W. Song et al., "The nature of Cu species in Cu-SAPO-18 catalyst for NH_3-SCR: combination of experiments and DFT calculations," *The Journal of Physical Chemistry C*, vol. 120, no. 27, pp. 14669–14680, 2016.

[27] C. Chen, Y. Cao, S. Liu, J. Chen, and W. Jia, "The catalytic properties of Cu modified attapulgite in NH_3-SCO and NH_3-SCR reactions," *Applied Surface Science*, vol. 480, pp. 537–547, 2019.

[28] C. Pang, Y. Zhuo, Q. Weng, and Z. Zhu, "The promotion effect of manganese on Cu/SAPO for selective catalytic reduction of NO_x with NH3," *RSC Advances*, vol. 8, no. 11, pp. 6110–6119, 2018.

[29] S. Han, J. Cheng, Q. Ye, S. Cheng, T. Kang, and H. Dai, "Ce doping to Cu-SAPO-18: enhanced catalytic performance for the NH_3-SCR of NO in simulated diesel exhaust," *Microporous and Mesoporous Materials*, vol. 276, pp. 133–146, 2019.